Combustion Science and Technology
Publication details, including instructions for authors and subscription information:
http://www.tandfonline.com/loi/gcst20

Experimental and Kinetic Modeling Study of the Combustion of n-Decane, Jet-A, and S-8 in Laminar Premixed Flames

Deepti Singh [a], Takayuki Nishiie [a] & Li Qiao [a]
[a] Department of Aeronautics and Astronautics, Purdue University, West Lafayette, Indiana, USA

Available online: 14 Sep 2011

To cite this article: Deepti Singh, Takayuki Nishiie & Li Qiao (2011): Experimental and Kinetic Modeling Study of the Combustion of n-Decane, Jet-A, and S-8 in Laminar Premixed Flames, Combustion Science and Technology, 183:10, 1002-1026

To link to this article: http://dx.doi.org/10.1080/00102202.2011.575420

Combust. Sci. and Tech., 183: 1002–1026, 2011

ISSN: 0010-2202 print/1563-521X online
DOI: 10.1080/00102202.2011.575420

Taylor & Francis
Taylor & Francis Group

EXPERIMENTAL AND KINETIC MODELING STUDY OF THE COMBUSTION OF n-DECANE, JET-A, AND S-8 IN LAMINAR PREMIXED FLAMES

Deepti Singh, Takayuki Nishiie, and Li Qiao
Department of Aeronautics and Astronautics, Purdue University, West Lafayette, Indiana, USA

Laminar flame speeds and Markstein lengths of n-decanelair, Jet-Alair, and S-8lair flames were measured using spherically expanding premixed flames. The experiment used a spherical combustion chamber housed inside a customized oven, which provides a uniform temperature distribution inside the chamber for fuel evaporation. Linear and nonlinear extrapolation methods to obtain unstretched flame speed were compared. The difference between linear and nonlinear extrapolation is within 0.3–2.0 cmls over the entire range of fuel equivalence ratio and decreases as the equivalence ratio increases. The measured flame speed data were compared to numerical simulations using several existing kinetic mechanisms and surrogate models. The results show that the JetSurF 0.2 mechanism was able to best represent the present measured flame speed data for n-decane. Surrogate models were simulated to represent the flame speeds of Jet-A and S-8. However, the simulated flame speeds overpredict the measured flame speeds. GC-MS and a negative ionization method were used to determine the composition change of the liquid fuels before and after heatinglvaporization. The result shows that when the initial temperature is above 500 K, auto-oxidation occurred during the mixing process for Jet-A and S-8 flames, which likely produced ketones or aldehydes, resulting in falsely lower flame-speed data.

Keywords: Chemical kinetics; Jet-A; Laminar flame speed; n-Decane; S-8; Surrogate models

INTRODUCTION

Understanding the detailed chemistry and combustion behavior of conventional and alternative fuels holds significance in the efficient utilization of these fuels in combustion systems. The chemistry of these real fuels, however, is extremely complicated because they typically involve many species. A promising approach toward modeling the combustion of complex fuels is to use "surrogate fuels" (Colket et al., 2007; Dagaut and Cathonnet, 2006; Farrell et al., 2007; Pitz et al., 2007). These fuels are a mixture of single-component fuels that can accurately reproduce the combustion-related gas phase chemical kinetics, transport, and physical properties of real fuels. Because fewer fuel compounds are involved, surrogates provide a cleaner and more reproducible basis for developing and testing the performance of practical

Received 2 November 2010; revised 7 March 2011; accepted 23 March 2011.
Address correspondence to Li Qiao, Assistant Professor, Department of Aeronautics and Astronautics, Purdue University, West Lafayette, IN 47907, USA. E-mail: lqiao@purdue.edu

combustors and for including detailed chemical kinetics in the analyses. Before these surrogates are used, though, it is important to validate the accuracy of the kinetics of single-component surrogates and the surrogate models used for representing real fuels. Significant efforts have been made in recent years to build a comprehensive experimental database for validation of the kinetics of single-component fuels and surrogate models.

Laminar flame speed is one of the most important parameters of a fuel/oxidizer mixture, which is an indication of the reactivity, diffusivity, and exothermicity of the mixture. Along with ignition delay time, laminar flame speed has been extensively studied as a parameter for the validation of chemical kinetics. Moreover, laminar flame speeds are also important in turbulent combustion modeling that uses laminar flamelet models. The most commonly used configurations for flame-speed measurements include counterflow flames, stagnation flames, and spherically expanding flames. With these classical apparatuses, flame speeds have been measured for major surrogate fuels, as well as for practical fuels that have drawn interest in recent years (Holley et al., 2006, 2007, 2009; Johnston and Farrell, 2005; Kelley and Law, 2009; Kelley et al., 2009; Kumar and Sung, 2007; Kumar et al., 2009; Skjøth-Rasmussen et al., 2003; Zhao et al., 2005). For instance, counterflow flames were used to study the propagation and extinction of large hydrocarbon fuels and real fuels (Holley et al., 2006, 2007, 2009; Ji et al., 2009; Kumar and Sung, 2007, 2009; Kumar et al., 2009). Spherically expanding flames have been used to measure flame speeds of C_5–C_8 alkanes at higher pressures and temperatures (Kelley and Law, 2009; Kelley et al., 2009, 2010).

In each of these experimental methodologies, flame speed is typically affected by stretch, and thus extrapolation is needed to obtain the unstretched flame speed. The linear extrapolation method proposed by Markstein (1964) and Clavin (1985), which assumes a linear relationship between the local flame speed and the stretch rate for small stretch rates based on asymptotic analysis, has been used extensively for simple fuels. It is highly sensitive to the geometry of the flame configuration as well as to the methodology used to obtain the temporal evolution of the flame front propagation speed and measurement range. Tahtouh et al. (2009) recently proposed a new methodology for linking the flame speed and the stretch linearly by introducing a Lambert function, which was shown to possess several advantages over the other methods. However, linear extrapolation is applicable only over a range that satisfies a strict set of assumptions. Nonlinear extrapolation may become necessary under conditions of high stretch rates or for mixtures with strong non-equidiffusion between fuel and oxidizer. Ji et al. (2009) proposed and implemented a new technique of nonlinear extrapolation for counterflow C_5–C_{12} alkane flames. This technique is based on a computed $S_{u,ref}$ vs. K correlation that considers detailed chemistry and variable transport coefficient, rather than the asymptotic analysis in which one-reactant, one-step kinetics are typically used. Their results confirmed that linear extrapolation resulted in higher flame-speed values than the nonlinear extrapolation method, especially for fuel-rich mixtures because of the large molecular weight discrepancy between the fuel and oxygen. Kelley et al. (Kelley and Law, 2009; Kelley et al., 2010) recently compared results obtained with linear and nonlinear extrapolations for iso-octane, n-heptane, n-butane/air, and hydrogen/air flames. Their results show that the use of linear extrapolation to determine laminar

speed could induce overpredictions by substantial amounts. They suggested that fidelity in the extraction of the laminar flame speed from expanding spherical flames can be facilitated by using small ignition energy and a large combustion chamber.

In addition to the extrapolation method, experimental challenges exist for the study of high-boiling-point and low-vapor-pressure fuels at elevated temperatures. One issue could be thermal decomposition, which would essentially change the composition of the reactant mixture and thus result in inaccurate values of the measured flame speed. Holley et al. (2006, 2007, 2009) described the fuel vaporization methodology used in the counterflow flames, in which the temperatures along the fuel-heating path were restricted within two limits: the lower limit was imposed by the requirement that the fuel is maintained in the gaseous phase, and the upper limit by the requirement that the fuel is not thermally decomposed. Another issue is the potential auto-oxidation of the heavier fuels when mixing with air for a period of time at higher temperatures. This concern may be more prevalent for spherically expanding flames than for counterflow flames; in the former, the air and fuel are allowed to mix for at least 10 minutes to ensure a homogeneous and quiescent mixture before ignition takes place. During this mixing period, auto-oxidation could occur, which again can vary the reactant mixture composition. Finally the flames of the heavier practical fuels will become sooty, emitting strong thermal radiation, and they may affect the representation/interpretation of flame speed if thermal radiation is unaccounted for in numerical simulations.

In the present study, we developed an experimentation method that uses spherically expanding flames for studying high-boiling-point, low-vapor-pressure fuels. The fuels studied here include n-decane, an important component of most surrogate mixtures models for jet fuels; Jet-A, a common aviation fuel; and S-8, a synthetic fuel derived from natural gas using the Fischer–Trospch process and consisting of several normal and branched alkanes (Edwards et al., 2004). The spherical combustion chamber, which has an inside diameter of 36 cm, is much larger than those used in previous studies (Kelley and Law, 2009; Kelley et al., 2009, 2010). The intention of using a large chamber was to decrease the nonlinear nature of flame response to stretch. The chamber was housed inside a customized oven to provide a uniform high temperature field for fuel vaporization. The experimental methodology, including the vaporization method, the flame speed extrapolation method, and the determination of the reactant mixture composition, has been validated and is described below. In particular, two fuel vaporization methods were used, and their effects on single fuels and fuel mixtures were compared. The methodology used to determine unstretched flame speed from the raw experimental data has been carefully addressed. The effects of linear and nonlinear extrapolation methods on flame speed have also been discussed. Further, the issue of potential thermal decomposition and auto-oxidation of the fuels was addressed using gas chromatography–mass spectrometry (GC-MS) and the negative ion chemical ionization method of GC-MS. Last, after validating the experimental methodology, we reported measurements of laminar flame speeds and the effects of flame stretch (represented by Markstein length) for the three fuels. We compared measurements for the single and multicomponent fuels with existing experimental data in the literature and with numerical simulations, using several existing reaction mechanisms and surrogate models.

EXPERIMENTAL METHODS

Apparatus

The experimental facility, as shown in Figure 1, consists of a spherical combustion chamber placed inside a customized oven, an electrode spark ignition system, a liquid fuel vaporization system, and a high-speed shadowgraph imaging system with a data-processing system. The spherical combustion chamber is made of stainless steel with an inner diameter of 36 cm. The method we used to determine flame speed is based on the assumption of flame propagation at constant pressure; thus the large volume of the combustion chamber allows us to use a wider range of flame radius for data extraction. The chamber is fitted with two diametrically opposed electrodes made of tungsten wires to achieve ignition at the center of the chamber. The position of the upper electrode is fixed, but the position of the lower electrode can be changed to adjust the distance of the gap between the two electrodes. The ignition energy is supplied from a high voltage power supply and adjusted to be near-minimum ignition energy to minimize ignition disturbances. The chamber has four ports on the top that provide connections for tubings, hoses, wires, and the fuel chamber. Quartz windows 10 cm in diameter and 1 cm thick are mounted on diametrically opposite ends of the chamber to allow viewing and recording the flame propagation within it.

The combustion chamber is placed inside a customized oven that can be preheated to a maximum temperature of 650°F with a precise temperature controller. This allows for vaporization of the liquid fuels and also provides capability for experiments at several initial temperatures of the fuel/oxidizer mixture. For optical access, the oven has large glass windows, one on the front door and one on the rear, which are aligned to the chamber windows. Two K-type thermocouples are installed to monitor the temperature inside the oven and the chamber, respectively. A uniform temperature field within the chamber can be achieved effectively using an oven.

A shadowgraph imaging system is set up to visualize flame propagation using a high-speed digital camera with a capture rate of up to 10,000 frames per second. The light source is a 100 W mercury lamp with a condensing lens and a pinhole. This

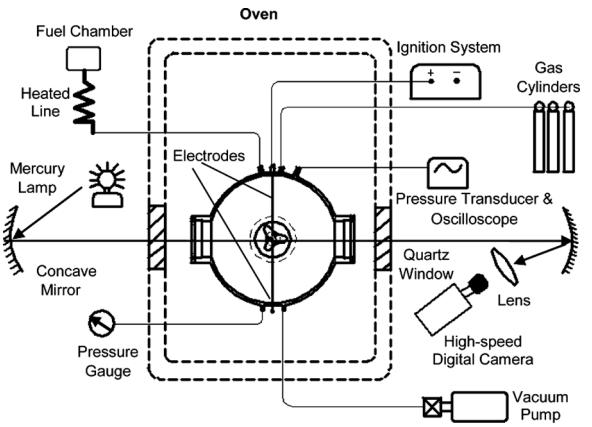

Figure 1 Schematic of the experimental facility.

provides sharp and intense illumination throughout the whole system. Two concave mirrors with a focal length of 1143 mm are placed on the two sides of the oven to focus the image on the camera.

Commercial grade compressed air with 99.5% purity was used for the experiment. n-Decane was purchased from Spectrum Chemicals and is assayed at 99% purity. Jet-A was procured from the Purdue Airport, and S-8 from the U.S. Air Force Research Laboratories.

Liquid Fuel Vaporization

The accuracy of the present results was based on the ability to vaporize the liquid fuels and to determine fuel/air equivalence ratios accurately. To achieve these goals, two different fuel injection methods are employed. The first involves vaporization of liquid fuels in 1/4-inch outer diameter stainless steel tubing wrapped in tape heaters. A temperature controller is used to stop the heater once the desired temperature is achieved. Several K-type thermocouples are installed along the surface of the fuel line to monitor the temperature and ensure uniform temperature distribution along the fuel line. The fuel vapor is then filled into the combustion chamber, using a precise valve based on the desired partial pressure of fuel vapor. The partial pressures of fuel vapor and oxidizer were monitored by two different Kulite high-temperature pressure gauges. Partial pressure of the fuel was measured with a high-accuracy gauge, which has a measurement range of 0–2 psi (XTEH-10L-190/S-1A). The other gauge has a larger measurement range of 0–50 psi (XTEH-7L-190-50A) and was used for monitoring the pressure of the total fuel–air mixture. Both pressure gauges can be operated at temperatures up to 650°F with an accuracy of 0.1% at the upper limit.

For heavier fuels, the partial pressures of fuel vapor are typically low under the present experimental conditions, e.g., the lowest partial pressure of n-decane is 0.1579 psi among all the tests at atmospheric pressure. This challenged accurate determination of the fuel–air equivalence ratio, even though a high-accuracy pressure gauge was used, because even a slight deviation of partial pressure could cause significant change in the fuel–air equivalence ratio. Because of this consideration, another fuel injection method was used to validate the fuel–air ratios; it was based on volume of the liquid fuel rather than on partial pressure of the fuel vapor. Liquid fuels were injected into the heated combustion chamber directly, using a 25-ml syringe (SGE Analytical Science) along with a syringe pump (KD Scientific, Model 1000 series). The syringe pump can be programmed to deliver the required amount of fuel volume with an accuracy of $\pm < 1\%$ and a repeatability of 0.1%. A 1/16-in diameter, 24-in long needle was used to deliver the fuel from the syringe to the combustion chamber through a Luer-Lok valve. The injection rate could be adjusted, and a low rate of 5 ml/h was chosen to allow faster evaporation of the droplets after a few trials. We observed that the droplets started to evaporate right after falling from the tip of the needle and became completely evaporated when they hit the hot combustion chamber wall.

The advantage of the first method is that the liquid fuel was prevaporized in a separate tank. Also, because the fuel line and the combustion chamber were preheated to the desired temperature, fuel condensation was not a major concern. However, the challenge was this: Because of the low partial pressure of the fuel vapor, the fuel equivalence ratio could be easily affected by small deviations in the input

quantity. In the second method, however, the fuel equivalence ratio was determined based on the volume of the liquid fuel, using a high-accuracy syringe pump. Complete vaporization of the fuel depended on the injection process. The two methods, however, produced almost the same results for pure liquid fuels, which is discussed in the following section. For multicomponent fuels, however, the results are different.

The test procedure began by heating the oven until the temperature inside the oven and chamber reached the target temperature. The combustion chamber and the fuel vaporization system were then evacuated by means of a vacuum pump. To avoid fuel condensation and ensure mixing, a small amount of air was added before we added fuel vapor to the chamber. After filling the desired amount of vapor based either on its partial pressure or on its volume, we added preheated air until the target pressure was achieved. The fuel–air mixture was allowed to stand for 10 min to ensure mixing and to allow the settling of any transient disturbances. The temperature and pressure inside the chamber were monitored during this period, and a drop in pressure, if any, was recorded. After each experiment, the chamber was flushed thoroughly with high-pressure air.

Data Processing

Similar to previous measurements of flame speeds (Qiao et al., 2005, 2007) for simple gaseous fuels using a spherical combustion chamber of the same size, flame radius measurements have been limited to a range of 12–15 mm $< r <$ 30 mm. The lower limit, which was determined experimentally for these fuels, was chosen to avoid disturbances caused by the transient ignition process; the upper limit was to ensure that the pressure increase inside the chamber was negligible. Under these assumptions, the local stretched flame speed and flame stretch is given by the following quasi-steady expressions proposed by Strehlow and Savage (1978),

$$S_L = \frac{\rho_b}{\rho_u}\frac{dr_f}{dt} \tag{1}$$

$$K = \frac{2}{r_f}\frac{dr_f}{dt} \tag{2}$$

where, S_L is the unburned gas speed and K is the flame stretch. The ratio of the burned gas to the unburned gas density was computed using the NASA Chemical Equilibrium Applications code assuming adiabatic constant pressure combustion (Gordon and McBride, 1994).

For small stretch rates, the stretched flame speed data can be extrapolated linearly to zero stretch to obtain the unstretched laminar flame speed, $S_{L\infty}$. The following equation proposed by Markstein (1964) and Clavin (1985) provides this linear relationship

$$S_L = S_{L\infty} - L_u K \tag{3}$$

where L_u is the Markstein length.

This linear relation [Equation (3)], however, is subject to the limitations of small stretch rate. Kelley and Law (2009) have clearly demonstrated a nonlinear behavior

for spherically propagating n-butane and other heavier hydrocarbon flames. Therefore, nonlinear extrapolation has also been studied here, and a comparison has been presented to show the extent of nonlinearity of the fuels being studied. The following nonlinear relation based on a model developed by Ronney and Sivashinsky (1989) specifically for quasi-steady, outwardly propagating spherical flames is used to obtain the unstretched laminar flame speed ($S_{b\infty}$)

$$\left(\frac{S_b}{S_{b\infty}}\right)^2 \ln\left(\frac{S_b}{S_{b\infty}}\right)^2 = -\frac{2L_bK}{S_{b\infty}} \tag{4}$$

where $S_{b\infty}$ and S_b are the unstretched and stretched flame speeds relative to burned gases, respectively. L_b is the burned gas Markstein length. The unstretched flame speed relative to unburned gases ($S_{L\infty}$) is related to $S_{b\infty}$ by the ratio of the burned and unburned gas densities. This model, which captures the nonlinear nature of these heavier hydrocarbons, is applicable over a larger range of flame radius where stretch rates can be moderately high.

Uncertainty Analysis

Uncertainties associated with the high-temperature pressure transducers used for the measurement of the partial pressures of fuel vapor and air are less than 0.1%. Additionally, uncertainties associated with the syringe pump system for delivering the desired amount of liquid fuel volume is within ±1%. Therefore, the uncertainty in the calculation of the fuel–air equivalence ratio is less than 1%. Further, experimental uncertainties (95% confidence) in the present flame radius and time intervals were estimated to be less than 3% and 1%, respectively. The corresponding uncertainties in dr_f/dt and K were less than 4.5% and 5.4%, respectively. The ratios of ρ_u/ρ_b were assumed to be known, so that they did not contribute to uncertainty estimates. This implies that the uncertainty in S_L was the same as that in dr_f/dt, and thus was less than 4.5%. Finally, the uncertainties in $S_{L\infty}$ and L were determined from the plots of S_L vs. K using the uncertainties of the intercept and slope, respectively. In general, the system uncertainty for $S_{L\infty}$ is found to be less than 10%. Moreover, for each flame condition, five to seven tests were conducted to minimize random errors in the experimentally determined flame speeds and in Markstein lengths.

The liquid fuels, including n-decane, Jet-A, and synthetic S-8, were tested at an initial temperature of 400 K over equivalence ratios varying from 0.7 to 1.6, and n-decane/O_2/He flames were considered by replacing nitrogen in the air with helium.

COMPUTATIONAL METHODS

Numerical simulations of the steady, laminar, freely propagating 1-D premixed flames were carried out using the PREMIX (Kee et al., 1985) module of the CHEMKIN (Kee et al., 1989) software. The multicomponent diffusion approximation was employed in the current simulations to calculate diffusion coefficients. The computational grid and the grid tolerance parameters in the simulations were lowered to values of 0.1 or lower where possible to ensure accuracy.

Several kinetic models exist to represent the ignition characteristics, oxidation, pyrolysis, and burning speeds of n-decane, including the mechanisms developed by Bikas and Peters (2001) (included in Honnet et al., 2009) and Zhao et al. (2005). Also available are large schemes, such as those by Sirjean et al. [JetSurF 0.2, (Sirjean et al., 2008)], Westbrook et al. (2009), and Ranzi et al. (2005). In the present work, simulations for n-decane flames have used the mechanisms by Zhao et al. (2005), Honnet et al. (2009), Ranzi et al. (2005), and the JetSurF 0.2 (Sirjean et al., 2008) model.

Jet-A is a mixture of many different hydrocarbons. Several surrogate models (e.g., Dean et al., 2007; Humer et al., 2007; Violi et al., 2002) have been proposed for Jet-A as well as for other kerosene-based jet fuels. Some of these models do not necessarily have the same physical properties but represent the chemical properties. Here, we used the six-component surrogate model that was suggested by Violi et al. (2002) for kerosene fuels. It includes 30% n-dodecane, 20% n-tetradecane, 10% iso-octant, 20% MCH, 15% o-xylene, and 5% tetralin. The Violi surrogate model was simulated using the comprehensive kinetic mechanism of Ranzi et al. (2005).

The surrogate model proposed by Natelson et al. (et al., 2008), which contains n-decane (53.1%) and iso-octane (46.9%), has been used to simulate S-8. It was simulated using the mechanisms of Ranzi et al. (2005).

RESULTS AND DISCUSSION

Data Processing Methodology and Linear/Nonlinear Extrapolation Methods

Previous studies have shown that for spherically expanding flames, several parameters such as ignition energy, transient evolution of the flame kernel, chamber confinement, compression-induced flow, and pressure rise can affect an accurate determination of unstretched flame speed. In the following, we will discuss the data processing methodology used in the present study. The flame was visualized using the software associated with a Phantom V7.3 high-speed camera. Each frame was processed individually, and the radius at each instant was recorded and plotted against time. Locally weighted scatterplot smoothing (LOWESS) was applied to the radius–time data to smooth it with a weighting function of 0.5. Figure 2 illustrates a typical radius vs. time evolution, showing raw and LOWESS-fitting data for a select range over which the flame can be assumed to propagate in a quasi-steady manner.

As mentioned earlier, flame radius used for data processing is generally limited to 12–15 mm $< r <$ 30 mm. Note that the combustion chamber used in the present study has an inner diameter of 360 mm. The upper limit of 30 mm was imposed on the radius of flame measurement in accordance with past flame speed measurement in a similar configuration (Aung et al., 1997; Hassan et al., 1998; Kwon et al., 1992; Qiao et al., 2005; Tseng et al., 1993). This value corresponds to 16.67% of the maximum radius and just 0.46% of the total volume of the chamber, which ensures that the pressure rise over this radius is less than 0.7%. Furthermore, Burke et al. (2009) and Chen et al. (2009a) show that for flame radius less than 40% of the maximum, the flame speed is affected by less than 1% because of a pressure increase in the chamber during flame propagation. In addition, a previous study by Faeth and co-workers (Kwon et al., 1992), using laser velocimeter measurements in a

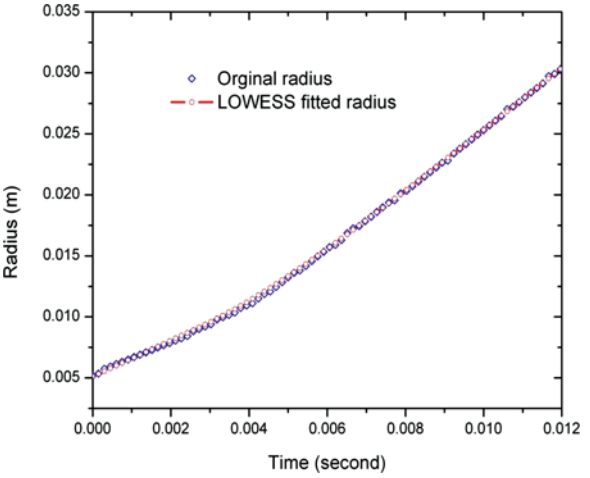

Figure 2 Typical radius-time evolution showing the original measured and LOWESS fitted data. (Figure is provided in color online.)

quasi-spherical chamber of inner diameter of 260 mm, showed that the velocity of the unburned gas within the chamber corresponded to the behavior expected of a freely propagating spherical laminar premixed flame. Thus it is safe to assume that the effects of motion in the burned gas and flow disturbances resulting from the presence of a chamber wall were small.

The lower limit of flame radii was established experimentally for these fuels to avoid ignition disturbances. In practice, we tried to minimize the ignition disturbances by using an energy that is near minimum ignition energy. However, with different amounts of ignition energy, the flames propagate at different rates in the initial period. Eventually, though, Chen et al. (2009b) showed theoretically that the flame will evolve at the same rate, regardless of ignition energy, after this initial region is affected by the ignition transients. These data free of the initial ignition effect should be taken into consideration for flame speed determination.

Figure 3 shows normalized burned gas-flame speed with respect to the stretch rate of the n-decane/air flames ($\phi = 1.0$) for three different ignition energies. The radius corresponding to the stretch rate, above which the behavior of the three flames is similar, was set as the lower limit. For the liquid fuels studied here, this limit was from 12–15 mm. An additional constraint on the lower limit comes from the assumption of an infinitely thin flame sheet applied in the derivation of the mathematical models to obtain unstretched laminar flame speed. The models hold only for instances where the ratio of the flame thickness to instantaneous flame radius is small ($\delta/r_f << 1$). Simulations for n-decane/air flames ($0.8 < \phi < 1.4$) based on the temperature profiles obtained from calculations using PREMIX yielded flame thicknesses of less than 0.6 mm. Therefore the lower radius limit of 12 mm sufficiently covers this constraint.

A final issue in the data processing methodology is the extrapolation method. As discussed earlier, nonlinear extrapolation may be necessary for heavier fuels because of the large differences in the diffusivity of these heavy hydrocarbon fuels

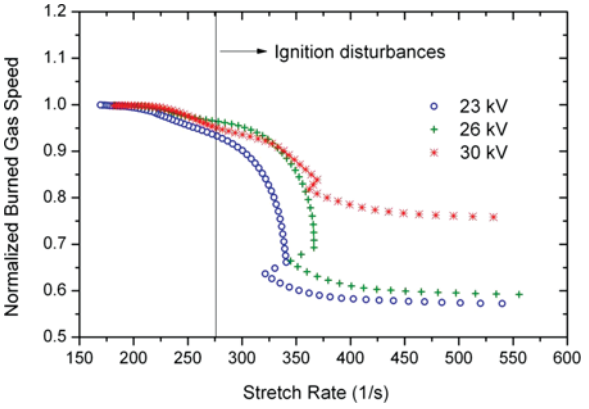

Figure 3 Normalized burned gas flame speed with respect to stretch rate for the n-decane/air flame ($\phi = 1.0$, P = 1 atm, T = 400 K) plotted for three different ignition energies. (Figure is provided in color online.)

and air. Motivated by this, we compared both linear and nonlinear extrapolation methods to determine unstretched flame speed. The nonlinear method [Equation (4)] based on the theoretical model of Ronney and Sivashinsky (1989) is specific to outwardly propagating flames and is not subject to small stretch limitations.

Figure 4 shows a comparison of flame speeds obtained by linear and nonlinear extrapolation for n-decane/air flames at various equivalence ratios. The linear extrapolation method overestimates flame speed in all three instances. The difference in the unstretched flame speeds obtained by linear and nonlinear extrapolation is within 0.3–2.0 cm/s for the three equivalence ratios, with the maximum difference occurring for $\phi = 0.8$. The difference decreases as the equivalence ratio increases. These findings are generally consistent with the results of Kelley and Law (2009), who found

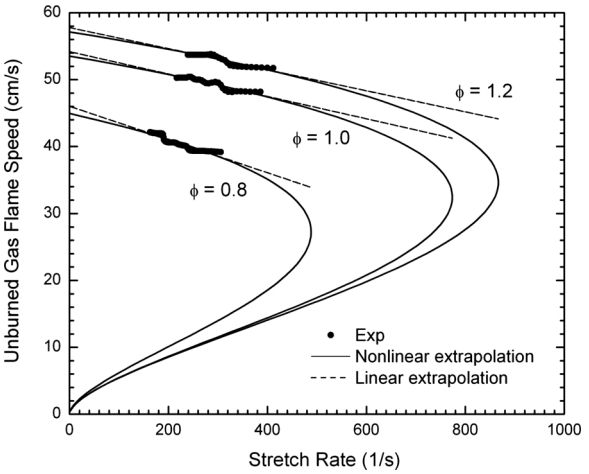

Figure 4 Comparison of flame speeds obtained by linear and nonlinear extrapolation for n-decane/air flames at 400 K and 1 atm.

that the difference between linearly and nonlinearly extracted flame speeds is from 1.4–3.4 cm/s for n-butane/air flames. The differences here, however, are smaller compared to those of Kelly and Law. This could be partially due to a relatively larger combustion chamber being used, which can reduce the nonlinear nature of flame response to stretch for the range of measurements being made. In the present experiment, flame radius was measured in the range of 15–30 mm, but this measurement was made in the range of 10–17 mm in the reference source, with the upper limit corresponding to a radius that is roughly 40% of the radius of the inner chamber.

Comparison of Two Fuel Vaporization Methods

Two different fuel vaporization methods that have been described earlier were used in the present experiment, and their effects were compared. In the first, the fuel–air equivalence ratio was determined by the partial pressure of fuel vapor and air. In the second method, liquid fuels were directly injected into the preheated combustion chamber, and the fuel–air equivalence ratio was determined by the volume of liquid being delivered. In the second method, partial pressures were also noted as verification for the equivalence ratio of the fuel–air mixture.

We compared the measured flame speeds of n-decane/air flames using these two methods. The results show that the difference in flame speeds from the two methods is negligible for all fuel-equivalence ratios. Therefore we can conclude that the volume method resulted in complete fuel vaporization and yielded an accurate determination of fuel–air equivalence ratio for the single-component liquid fuel studied here.

For multicomponent fuels such as Jet-A, however, the measured flame speeds using the two methods show significant deviations, as seen in Figure 5. The deviation is significant on the fuel-lean side, but it is almost negligible under fuel-rich conditions.

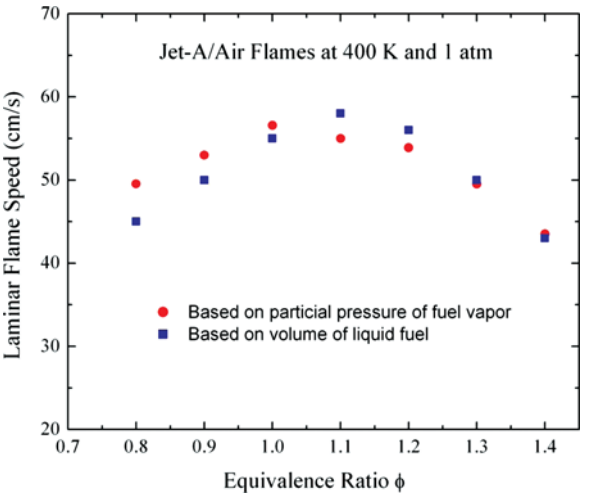

Figure 5 Comparison of laminar flame speeds obtained from two fuel vaporization methods for Jet-A/air flames at 400 K and 1 atm. (Figure is provided in color online.)

The deviation is greater than the experimental uncertainties and therefore must be considered while experiments for practical fuels with multiple components are being performed. Because Jet-A contains multiple species when heated inside the fuel chamber and transported through the fuel line, preferential evaporation will occur: The species with lower boiling points may escape first and faster than those with higher boiling points. Additionally, the distillation curve of Jet-A samples typically exists between 410 K and 577 K. The lower end is very close to the experimental condition. Thus the original fuel and the vaporized fuel transported into the combustion chamber might have had different compositions. The vaporized fuel could thus contain more species of lower boiling points, which generally have higher burning speeds, resulting in higher flame-speed data, as shown in Figure 5. However, in the direct fuel-injection method, complete evaporation occurred inside the chamber; thus no such phenomenon could have occurred. For multicomponent fuels, therefore, the volume-based method to determine the fuel–air ratio is more accurate and was used in the present study.

Unstretched Laminar Flame Speed

Experiments were carried out at an initial temperature of 400 K and an initial pressure of 1 atm for n-decane/air, Jet-A/air, and S-8/air mixtures at various fuel equivalence ratios. Further, n-decane/oxygen flames were further studied with helium (He) dilution. Flame speeds were measured as discussed earlier and were based on the nonlinear extrapolation method. They were compared with predictions using several existing mechanisms and with experimental results from the literature. These results are presented below.

n-Decane/air flames. n-Decane is one of the major straight-chain components of kerosene, and is included as an important component of most surrogate mixture models. Figure 6 shows the measured and predicted laminar flame speeds of n-decane/air flames as a function of equivalence ratio for a range of 0.8–1.4 at 400 K and 1 atm. The upper limit of $\phi = 1.4$ on the experiments was imposed by the early development of instabilities, which limited the data available for flame-speed extrapolation. Below $\phi = 0.8$, the flames were very weak, and that made measuring flame-speed difficult. Simulation results presented were obtained using the mechanisms of Zhao et al. (2005), Honnet et al. (2009), Ranzi et al.(2005), and the JetSurF 0.2 (Sirjean et al., 2008). Also shown in Figure 6 are the experimentally determined flame speeds by Kumar and Sung (2007) and Ji et al. (2009), both using counterflow flame configurations. Experiments conducted by Kumar and Sung (2007) were at 400 K and 1 atm, and those by Ji et al. (2009) were at 403 K and 1 atm.

The present measured flame speeds using the spherical chamber are in good agreement with the results of Ji et al. (2009) that were made in a counterflow apparatus, except in the region near the stoichiometric condition. The largest discrepancy occurs near stoichiometric conditions with the present data being 3–5 cm/s lower. The flame speeds measured by Kumar and Sung (2007), also in a counterflow arrangement, increasingly deviate from the measurements of Ji et al. (2009) in the fuel-rich region. The former used linear extrapolation in the determination of unstretched flame speed, and the latter implemented the use of a nonlinear extrapolation method

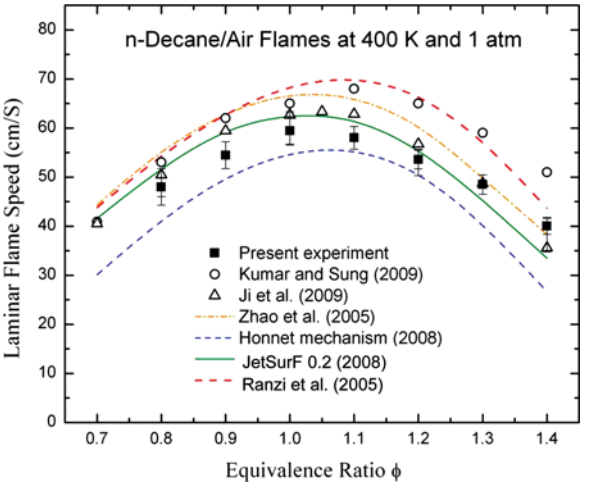

Figure 6 Measured and predicted laminar flame speeds of n-decane/air flames as a function of equivalence ratio at 400 K and 1 atm. The lines in the diagram represent simulation results; the symbols represent experimental results. (Figure is provided in color online.)

based on the method of Wang et al. (2009), which may be responsible for the differences between the two measurements under the fuel-rich conditions where the Lewis number effect becomes significant.

Considerable variation between predictions by the four mechanisms is seen in Figure 6. The JetSurf 0.2 mechanism most closely represents experimental data of Ji et al. (2009) and present measurements over the entire range of equivalence ratios. Predicted flame speeds using the mechanism by Honnet et al. (2009) highly underpredict measured flame speeds in the fuel-lean region and the fuel-rich region. Flame-speed predictions using the Ranzi et al. (2005) mechanism are good under fuel-lean conditions, but they significantly overpredict the present data in the fuel-rich regions. Numerical simulations using the Zhao et al. (2005) mechanism slightly overpredict data over most of the range under study here.

The present measurements are slightly lower than those obtained with counterflow flames at most fuel-equivalence ratios, even though we have used two fuel vaporization methods to ensure accuracy of fuel equivalence ratios for n-decane/air flames. The observed discrepancies could be due to differences in the experimental configurations when testing heavier fuels, i.e., spherically expanding flames vs. counterflow flames. Differences in the results from these two configurations have also been observed previously by Farrell et al. (2004). The reason for this discrepancy, though it has yet to be qualitatively explained, could be due to the interpretation of the experimental data, especially the definition and determination of the unstretched flame speed for various flow configurations. For instance, the difference could be inherent to the extrapolation methodology from stretched flame speed data and essentially different stretch effects seen in the two configurations.

Jet-A/air flames. Figure 7 shows the measured and numerically predicted flame speed of Jet-A/air flames as a function of equivalence ratio for a range of

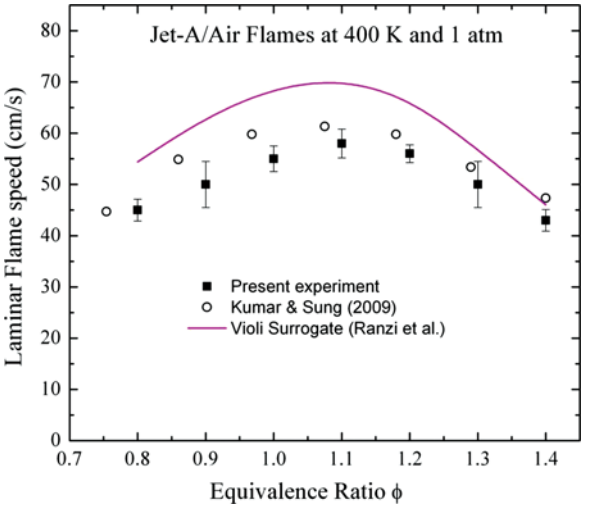

Figure 7 Measured and predicted laminar flame speeds of Jet-A/air flames as a function of equivalence ratio at 400 K and 1 atm. The lines represent simulations, and the symbols represent experimental results. (Figure is provided in color online.)

0.7–1.4 at 400 K and 1 atm. The physical characteristics of Jet-A, including air-to-fuel ratio and molar mass, were determined based on the 12-component surrogate model by Schulz (1991). This physical surrogate mixture proposed by Schulz (1991) has an average molecular weight of 147.83 g/mol, a hydrogen-to-carbon ratio of 1.91, and an average chemical formula of $C_{10.6}H_{20.2}$. Most fuel components are straight-chain alkanes (60%) and aromatics (20%), and the remaining 20% are cycloalkanes and branched alkanes.

A comparison of the measured flame speeds have been made with the numerical simulations using the Violi surrogate model (Violi et al., 2002). The only available literature data on the laminar flame speeds of Jet-A were reported by Kumar et al. (2009). Similar to the results for n-decane/air flames, the present measurements are slightly lower than those of Kumar et al. (2009) made by using the counterflow configuration. The maximum flame speed occurs at approximately the same equivalence ratio ($\phi = 1.1$). Maximum deviation between these experimental values occurs near the stoichiometric condition and has a magnitude close to 6% (<5 m/s lower).

Because of the large number of alkanes and a significant proportion of aromatics present in the fuel, Jet-A has a greater propensity to sooting than n-decane does. Heavy sooting was observed, especially for stoichiometric and rich flames. Carbon residues were left on the windows and on the wall of the chamber. The presence of soot, which causes radiation heat losses, may reduce flame temperature and therefore flame speed. Also, because these flames are slow, volumetric heat loss from the burned gases could also be significant, as posited theoretically by Chen and Ju (2007). Spherical flames possibly have greater heat loss as compared with counterflow setups because of the larger volume of burned gases for radiative heat loss. The numerical simulations, however, considered adiabatic flames. Nevertheless, more investigation is needed to quantitatively understand the effect of soot radiation in such flames. Another factor that might affect the results is that the composition of

Jet-A varies widely from source to source. Also, storage of these fuels for extended periods results in oxidative degradation of the fuel.

The surrogate model proposed by Violi et al. (2002) simulated with the kinetics of Ranzi et al. (2005) predicts higher flame speeds than the measured values, and this difference is particularly prominent under stoichiometric conditions. As can be seen from Figure 7, the Ranzi et al. (2005) kinetics overpredict the flame speeds even for n-decane. Therefore, the overprediction seen here to some extent can be a result of the kinetic mechanism used.

S-8/air flames. S-8 is a synthetic jet fuel, a mixture of several normal and branched alkanes, that is derived from natural gas using the Fischer–Tropsch process (Huber et al., 2008). Determination of the fuel equivalence ratios and the density of unburned gases was based on the seven-component S-8 thermophysical surrogate model proposed by Huber et al. (2008). This surrogate mixture has an average molar mass of 161.74, an H/C ratio of 2.17, and an average chemical formula of $C_{11.4}H_{24.8}$ containing about 38% of straight chain alkanes and 62% of branched alkanes.

Figure 8 shows the measured and predicted laminar burning speed of S-8/air flames as a function of equivalence ratio for a range of 0.7–1.4 at 400 K and 1 atm. To the best of our knowledge, the literature has only one existing chemical surrogate proposed for F-T derived S-8. This surrogate model proposed by Natelson et al. (2008) contains n-decane (53.1%) and iso-octane (46.9%). It was simulated using the mechanisms of Ranzi et al. (2005). Also shown are the measured flame speeds by Kumar et al. (2009b) using counterflow flames. Similar to the n-decane/air flames and the Jet-A/air flames in Figures 6 and 7, the present measurements are slightly lower than those of Kumar et al. (2009). Also, the equivalence ratio at which the maximum flame speed was obtained is 1.05 for the present case, which is slightly toward the lean side of the peak equivalence ratio obtained for Kumar et al.

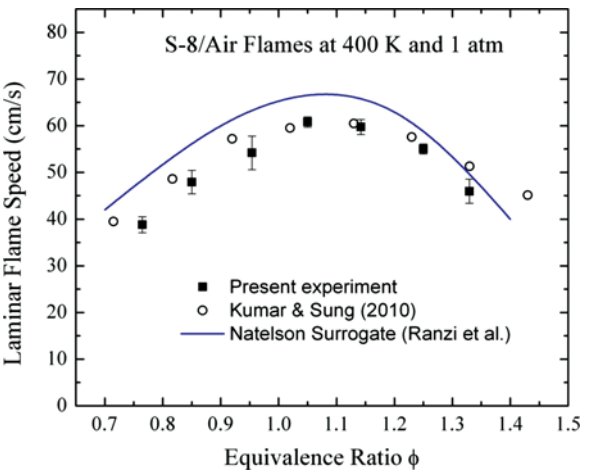

Figure 8 Measured laminar flame speeds of S-8/air flames as a function of equivalence ratio at 400 K and 1 atm. The line represents simulations, and the symbols represent experimental results. (Figure is provided in color online.)

(2009). The present measurements and the simulation results using the Natelson surrogate model have better agreement in the fuel-rich region than in the fuel-lean region.

Flame speed comparisons of n-decane/air, Jet-A/air, and S-8/air flames. The measured flame speeds of n-decane/air, Jet-A/air, and S-8/air were compared in Figure 9 as a function of fuel equivalence ratio at 400 K and 1 atm. A difference of flame speeds is found between n-decane and the two other fuel mixtures, particularly on the fuel-lean side. n-Decane has marginally higher flame speeds over the fuel-lean side. Under stoichiometric and fuel-rich conditions, the flame speeds of the three fuels lie within the range of experimental uncertainties of one another. The maximum flame speeds of Jet-A and S-8 are shifted to a slightly fuel-rich ratio in comparison to that of n-decane. These differences are a result of the fuel compositions. Jet-A has a significant proportion of aromatics, and S-8 has a significant composition of branched alkanes that tend to have lower flame speeds than n-alkanes. Additionally, aromatics have lower flame speeds than alkanes, as shown by Davis et al. (1996). Thus, the mean flame speeds of Jet-A are lower than those of S-8 on the fuel-lean side.

Effect of helium dilution. Within spherical expanding flames, preferential diffusion effects result in the creation of a wrinkled flame surface for heavy (or light) fuel molecules, such as n-decane (or hydrogen) under fuel-rich (or fuel-lean) conditions. To increase the range of measurements, that is, to delay the development of preferential-diffusion instabilities, we replaced N_2 with helium, which has a much smaller molecular weight. Early development of flame instabilities was not observed in these flames; thus flame speed measurements could be made easily over a larger range of equivalence ratios on the fuel-rich side. This helped to extend the range of equivalence ratios over which the unstretched laminar burning speeds could be measured.

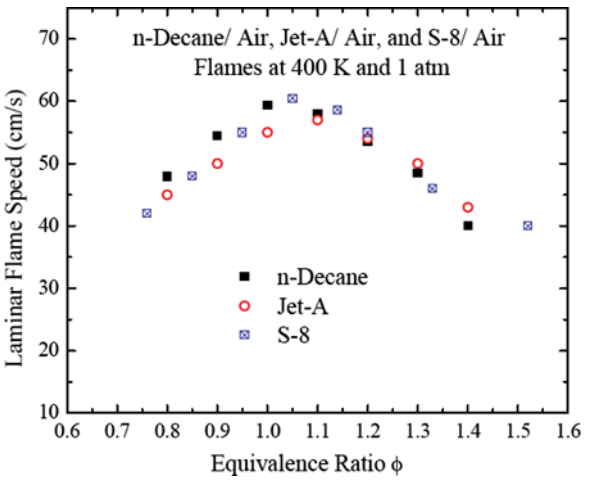

Figure 9 Comparison of measured laminar flame speeds of n-decane/air, Jet-A/air, and S-8/air at 400 K and 1 atm. (Figure is provided in color online.)

The flame speeds of n-decane/O_2/He were examined at an initial temperature of 400 K and pressure of 1.0 atm for the equivalence ratio of 1.0–1.6, as shown in Figure 10. The O_2 and He were mixed in the ratio of O_2:He = 1:3.76. The present experimental results were compared with the computational results, using the mechanism by Zhao et al. (2005) and the JetSurF 0.2. (Sirjean et al., 2008). The result shows that the predicted flames speeds using the two mechanisms are in good agreement with the measured flame speeds for n-decane/O_2/He over all the equivalence ratios ($\phi = 1.0 \sim 1.6$). Compared to the n-decane/air flame, the flame speeds of n-decane/O_2/He were almost four times higher, primarily because of higher transport rates and the lower heat capacity of helium. Also observed in the experiments were the relatively higher ignition energies required to ignite the helium-diluted flames than the nitrogen-diluted flames.

Markstein Length

The chief advantage of using a spherical flame configuration is an easier and straightforward measurement of flame speed and stretch rate as in comparison to other experimental configurations. Therefore the Markstein length can be easily obtained (Strehlow and Savage, 1978). It is a direct measure of the flame response to stretch and an important parameter to assess the stability of the flames to preferential diffusion effects. The fuels considered here have large molecular weights, and the present results are different from those observed in past studies on lighter hydrocarbons. Figure 11 shows the Markstein lengths for n-decane/air, Jet-A/air, and S-8/air mixtures at 1 atm and 400 K. A decrease in Markstein lengths is observed for all three fuels with an increase in equivalence ratios, and a transition to negative values occurs at an equivalence ratio of 1.2 for n-decane/air and approximately 1.3 for Jet-A/air and

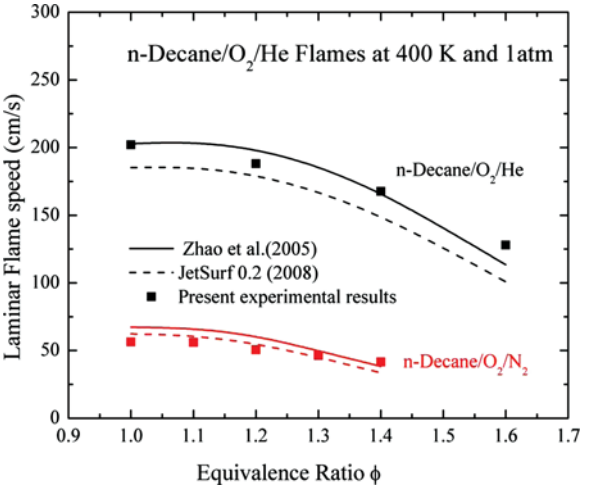

Figure 10 Measured and predicted laminar flame speeds of n-decane/O_2/N_2 and n-decane/O_2/He flames as a function of equivalence ratio at 400 K and 1 atm. The lines represent simulations, and the symbols represent experimental results. (Figure is provided in color online.)

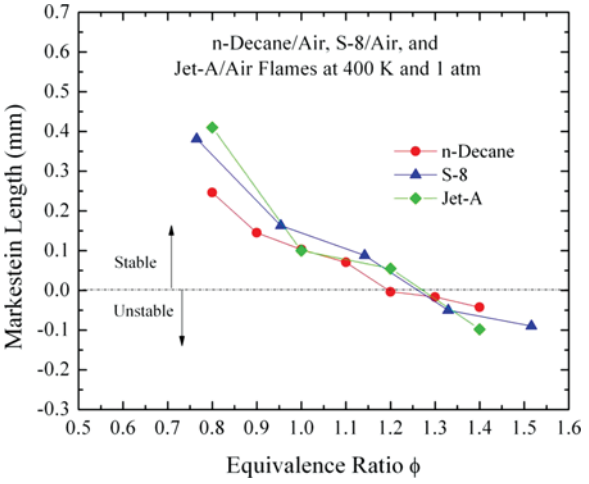

Figure 11 Measured Markstein lengths of n-decane/air, Jet-A/air, and S-8/air flames as a function of fuel equivalence ratio at 400 K and 1 atm. (Figure is provided in color online.)

S-8/air flames. Negative values of Markstein length indicate unstable flames and increased preferential diffusion instabilities. This trend of Markstein lengths is opposite to observations made for H_2/air flames (Aung et al., 1997). For n-decane/air and Jet-A/air flames, the development of flame instabilities was too soon to allow enough measurements to be made for flames beyond $\phi = 1.4$. S-8/air flames were slightly more stable than n-decane and Jet-A/air flames, and flame speeds could be measured until $\phi = 1.5$.

Markstein lengths of n-decane/O_2/He were compared with n-decane/O_2/N_2 in Figure 12. The Markstein lengths are approximately three times higher for He-diluted

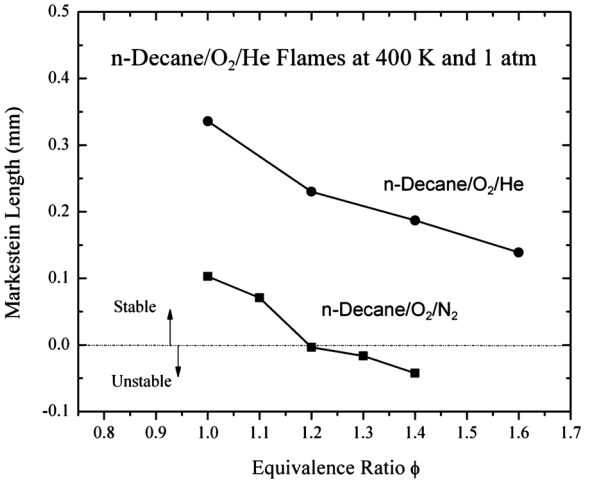

Figure 12 Measured Markstein lengths of n-decane/O_2/N_2 and n-decane/O_2/He flames as a function of equivalence ratio at 400 K and 1 atm.

mixtures in comparison to N_2-diluted mixtures. Flames studied over equivalence ratios of 1.0–1.6 for n-decane/O_2/He are stable over the entire range, whereas the n-decane/O_2/N_2 flames become unstable at $\phi = 1.2$. Such a great difference in response to stretch is attributed to the large diffusivity of helium.

GC/MS Analysis of the Reactant Mixture Composition

The vaporization of liquid fuels along with the accurate determination of fuel-air equivalence ratios is a challenging process, which is especially true for practical fuels that contain multiple species. The temperature of the combustion chamber and the fuel system must be maintained at appropriate values to avoid fuel condensation and thermal decomposition. Besides thermal decomposition, another concern is auto-oxidation of the fuels because of the long duration (at least 10 min) of fuel vapor in the combustion chamber at elevated temperatures during the mixing process. Even though very low reactivity has been observed for most heavy hydrocarbon fuels below 600 K, if a certain degree of thermal decomposition and auto-oxidation occurs, it will affect the appropriate interpretation of the experimental data because of change in the reactant mixture composition. The degree of thermal decomposition and auto-oxidation depends on the temperature, flow residence time, and specific fuel being tested. Therefore it was essential to validate the reactant mixture composition of each fuel at each initial temperature to ensure accurate flame speed data.

For n-decane, thermal decomposition and auto-oxidation are unlikely to be an issue under present experimental conditions (1 atm, 400 K), as also evidenced by previous studies due to its higher boiling point and autoignition point. Therefore the discussion here will focus on Jet-A and S-8.

Jet-A is a multicomponent fuel with several different hydrocarbons; it was essential to ensure that the reactant mixtures after mixing and before ignition were the same as in liquid Jet-A. GC-MS was used to determine the constituents of the fuel under various conditions to ensure that thermal decomposition and auto-oxidation did not occur in the heated combustion chamber during the mixing process. A mass spectrum analysis of a fresh sample of Jet-A and a heated sample of Jet-A vapor from the chamber were conducted to determine the major components of the fuel before and after heating. To examine the possible change of fuel compositions at those times, the Jet-A/air mixture inside the chamber was extracted 45 min after it was filled at 400 K and 1 atm.

Figure 13 shows the mass spectrum of Jet-A liquid and vapor. Each figure has several large peaks, and the concentration of each chemical species is related to the area under the respective peaks. The five peaks in Figure 13 represent the major components of Jet-A fuel. No significant differences were observed in the mass spectrum analyses of these two samples, indicating that there was no change in the fuel composition. A similar analysis done at an initial temperature of 500 K indicated that the liquid and fuel vapors have obvious differences in their compositions; thus thermal decomposition and auto-oxidation could be a problem at temperatures higher than 500 K for Jet-A. This has also been demonstrated by a few past studies (Jones and Balster, 1999; Jones et al., 1998; You et al., 2009).

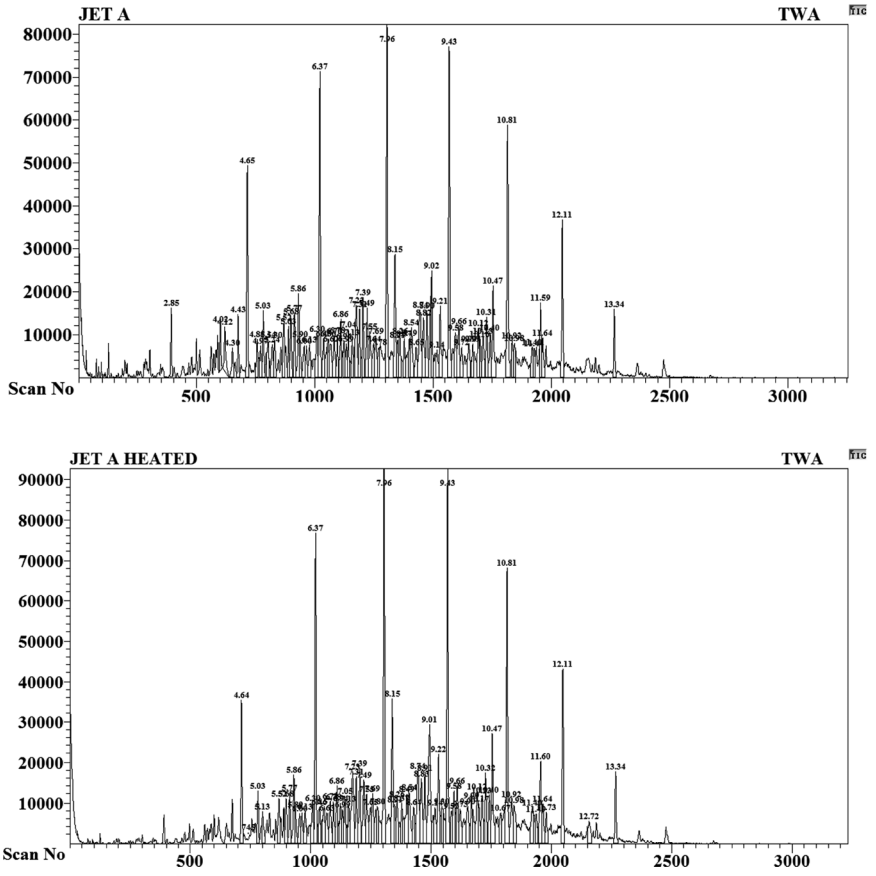

Figure 13 Mass spectrum–gas chromatography analysis of Jet-A: liquid at 298 K (top) and vapor at 400 K (bottom).

Furthermore, if a small amount of oxidation occurred at that temperature, an outstanding difference in concentration might not be observed in the GC/MS analysis. For this reason, additional tests were done by use of a negative ionization method (Figure 14), which is more effective in detecting oxygenated species. For this test, three samples were used, including the two samples described above. The third was prepared similarly to the earlier sample by heating the fuel/air mixture to a temperature of 500 K, cooling down the chamber after 45 min, and then collecting the liquid sample, using hexane as a solvent. The negative ion GC/MS test showed distinct peaks of species with molecular weights of 148, 162, 176, and 190 in its analysis of the 500 K sample. These peaks differed by a molecular weight of 14, which is most likely indicative of CH_2 branches. The molecular weights of these peaks are very likely to correspond to ketones or aldehydes, which are observed in the oxidation process of these hydrocarbons. Actually, flame speed measurement experiments were attempted at 500 K and 1 atm for stoichiometric compositions, and surprisingly low flame speeds ($\sim$25 cm/s) were obtained, which are counterintuitive to what is

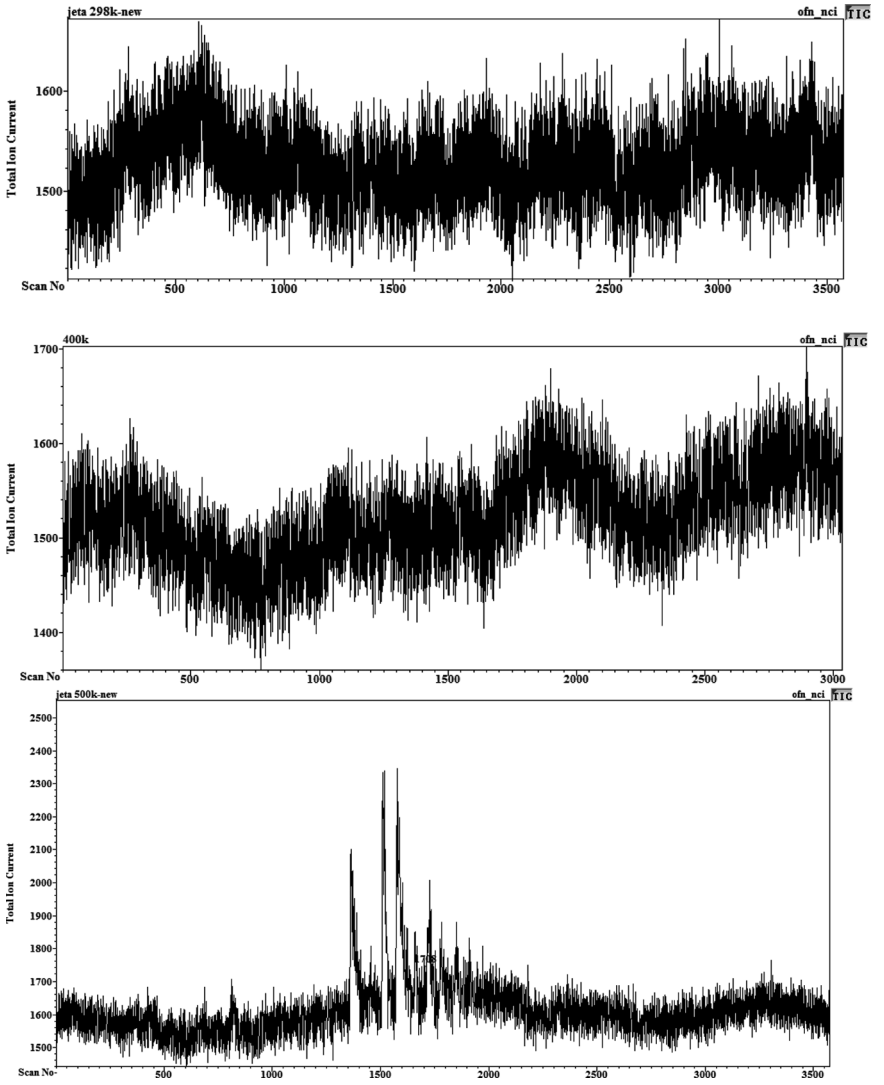

Figure 14 Mass spectrum–gas chromatography using negative ionization analysis of Jet-A: liquid at 298 K (top), vapor at 400 K (middle), and vapor at 500 K (bottom).

expected with increasing temperatures. On the other hand, no such peaks were seen for the 400 K heated sample and the untouched sample stored at 298 K.

From this analysis, it can be said with certainty that thermal decomposition or auto-oxidation did not occur under the present experimental conditions for the fuels studied here, nor did they interfere with the flame speed measurements. However, care must be taken when experiments are conducted at higher temperatures in different setups, e.g., greater than 500 K, since auto-oxidation can result in a change of the reactant mixture composition, thus lowering the actual flame speeds.

CONCLUSIONS

Laminar flame speeds and Markstein lengths of n-decane/air, Jet-A/air, and S-8/air flames were measured using spherically expanding premixed flames in a preheated combustion chamber. Following are the prominent conclusions:

1. The differences (0.3–2.0 cm/s) in unstretched flame speed obtained by linear and nonlinear extrapolation methods are smaller compared to those in the literature also using spherical flames, largely because a relatively larger combustion chamber was used, which can reduce the nonlinear nature of flame response to stretch.
2. The fuel equivalence ratios determined on the basis of the volume method were found to be more accurate than the partial pressure method for multicomponent fuels because of the tendency of preferential evaporation of the lower-boiling-point species in the reactant mixture using the latter method.
3. The JetSurF 0.2 mechanism was able to best represent the present measured flame-speed data for n-decane/air flames. For Jet-A/air flames, flame speeds simulated by the Violi et al. (2002) surrogate using the mechanism of Ranzi et al. (2005) overpredicted the measured flame speeds. Comparison of the flame speeds for Jet-A, synthetic jet fuel S-8, and n-decane showed similarities in their combustion behavior with some differences on the fuel-lean side, which arose primarily due to the presence of aromatics in Jet-A and branched alkanes in S-8.
4. Measured flame speeds from the present spherically expanding flame configuration are a few cm/s lower than similar measurements made in a counterflow apparatus. This could be due to the interpretation of the experimental data, especially the extrapolation methods. Moreover, radiation heat loss from soot, notably for the fuels that contain a large portion of aromatics, requires further investigation.
5. Last, composition analysis using GC-MS and a negative ionization method shows that thermal decomposition or auto-oxidation did not occur under the present experimental conditions (400 K, 1 atm) for the fuels studied here. But when the initial temperature is above 500 K, auto-oxidation occurred during the mixing process, which likely produced ketones or aldehydes, and resulted in a falsely lower flame speed because of composition change of the reactant mixture.

REFERENCES

Aung, K.T., Hassan, M.I., and Faeth, G.M. 1997. Flame stretch interactions of laminar premixed hydrogen/air flames at normal temperature and pressure. *Combust. Flame*, **109**, 1–24.

Bikas, G., and Peters, N. 2001. Kinetic modelling of n-decane combustion and autoignition: Modeling combustion of n-decane. *Combust. Flame*, **126**, 1456–1475.

Burke, M.P., Chen, Z., Ju, Y.G., and Dryer, F.L. 2009. Effect of cylindrical confinement on the determination of laminar flame speeds using outwardly propagating flames. *Combust. Flame*, **156**, 771–779.

Chen, Z., Burke, M.P., and Ju, Y. 2009a. Effects of compression and stretch on the determination of laminar flame speeds using propagating spherical flames. *Combust. Theor. Model.*, **13**, 343–364.

Chen, Z., Burke, M.P., and Ju, Y.G. 2009b. Effects of Lewis number and ignition energy on the determination of laminar flame speed using propagating spherical flames. *Proc. Combust. Inst.*, **32**, 1253–1260.

Chen, Z., and Ju, Y. 2007. Theoretical analysis of the evolution from ignition kernel to flame ball and planar flame. *Combust. Theor. Model.*, **11**, 427–453.

Clavin, P. 1985. Dynamic behavior of premixed flame fronts in laminar and turbulent flows. *Prog. Energy Combust. Sci.*, **11**, 1–59.

Colket, M., Edwards, T., Williams, S., Egolfopoulos, F., Lindstedt, P., Pitsch, P., Seshadri, K., Dryer, F.L., Law, C.K., Friend, D., Lenhert, D.B., Sarofim, A., Smooke, M., and Tsang, W. 2007. Development of an *Experimental Database and Kinetic Models for Surrogate Jet Fuels*. Presented at the 45th AIAA Aerospace Sciences Meeting and Exhibit, Jan. 8–11, Reno, NV.

Dagaut, P., and Cathonnet, M. 2006. The ignition, oxidation, and combustion of kerosene: A review of experimental and kinetic modeling. *Prog. Energy Combust. Sci.*, **32**, 48–92.

Davis, S.G., Wang, H., Brezinsky, K., and Law, C.K. 1996. Laminar flame speeds and oxidation kinetics of benzene-air and toluene-air flames. *Proc. Combust. Inst.*, **26**, 1025–1033.

Dean, A.J., Penyazkov, O.G., Sevruk, K.L., and Varatharajan, B. 2007. Autoignition of surrogate fuels at elevated temperatures and pressures. *Proc. Combust. Inst.*, **31**, 2481–2488.

Edwards, T., Minus, D., Harrison, W., Corporan, E., Dewitt, M., Zabarnick, S., and Balster, L. 2004. Fischer–Tropsch jet fuels—characterization for advanced aerospace applications. Presented at the 40th AIAA/ASME/SAE/ASEE Joint Propulsion Conference and Exhibit, July 11–14, Fort Lauderdale, Florida.

Farrell, J.T., Cernansky, N.P., Dryer, F.L., Friend, D.G., Hergart, C.A., Law, C.K., Mc David, R.J.M.C., and Pitsch, H. 2007. Development of an experimental database and kinetic models for surrogate diesel fuels. Presented at the 2007 SAE World Congress, April 16–19, Detroit, MI.

Farrell, J.T., Johnston, R.J., and Androulakis, I.P. 2004. Molecular structure effects on laminar burning velocities at elevated temperature and pressure, Presented at the 2004 SAE World Congress, March 1–5, Detroit, MI.

Gordon, S., and McBride, B.J. 1994. Computer Program for Calculation of Complex Chemical Equilibrium Compositions and Applications, Part I: Analysis, NASA RP-1311.

Hassan, M.I., Aung, K.T., Kwon, O.C., and Faeth, G.M. 1998. Properties of laminar premixed hydrocarbon/air flames at various pressures. *J. Propul. Power*, **14**, 479–488.

Holley, A.T., Dong, Y., Andac, M.G., and Egolfopoulos, F.N. 2006. Extinction of premixed flames of practical liquid fuels: Experiments and simulations. *Combust. Flame*, **144**, 448–460.

Holley, A.T., Dong, Y., Andac, M.G., Egolfopoulos, F.N., and Edwards, T. 2007. Ignition and extinction of non-premixed flames of single-component jet fuels, and liquid hydrocarbons, their surrogates. *Proc. Combust. Inst.*, **31**, 1205–1213.

Holley, A.T., You, X.Q., Dames, E., Wang, H., and Egolfopoulos, F.N. 2009. Sensitivity of propagation and extinction of large hydrocarbon flames to fuel diffusion. *Proceed. Combust. Inst.*, **32**, 1157–1163.

Honnet, S., Seshadri, K., Niemann, U., and Peters, N. 2009. A surrogate fuel for kerosene. *Proc. Combust. Inst.*, **32**, 485–492.

Huber, M.L., Smith, B.L., Ott, L.S., and Bruno, T.J. 2008. Surrogate mixture model for the thermophysical properties of synthetic aviation fuel S-8: Explicit application of the advanced distillation curve. *Energy Fuels*, **22**, 1104–1114.

Humer, S., Frassoldati, A., Granata, S., Faravelli, T., Ranzi, E., Seiser, R., and Seshadri, K. 2007. Experimental and kinetic modeling study of combustion of JP-8, its surrogates and reference components in laminar nonpremixed flows. *Proc. Combust. Inst.*, **31**, 393–400.

Ji, C., Dames, E., Wang, Y.L., Wang, H., and Egolfopoulos, F.N. 2009. Propagation and extinction of premixed C5–C12 n-alkane flames. *Combust. Flame*, **157**, 277–287.

Johnston, R.J., and Farrell, J.T. 2005. Laminar burning velocities and Markstein lengths of aromatics at elevated temperature and pressure. *Proc. Combust. Inst.*, **30**, 217–224.

Jones, E., and Balster, L. 1999. Autoxidation of dilute jet-fuel blends. *Energy Fuels*, **13**, 796–802.

Jones, E., Balster, L., and Balster, W. 1998. Autoxidation of neat and blended aviation fuels. *Energy Fuels*, **12**, 990–995.

Kee, R.J., Grcar, J.F., Smooke, M.D., and Miller, J.A. 1985. *A FORTRAN Program for Modeling Steady Laminar One-Dimensional Premixed Flames*, Sandia National Laboratories, Livermore, CA.

Kee, R.J., Rupley, F.M., and Miller, J.A. 1989. *Chemkin-II: A FORTRAN Chemical Kinetics Package for the Analysis of Gas-Phase Chemical Kinetics*, Sandia National Laboratories, Livermore, CA.

Kelley, A.P., Jomaas, G., and Law, C.K. 2009. Critical radius for sustained propagation of spark-ignited spherical flames. *Combust. Flame*, **156**, 1006–1013.

Kelley, A.P., and Law, C.K. 2009. Nonlinear effects in the extraction of laminar flame speeds from expanding spherical flames. *Combust. Flame*, **156**, 1844–1851.

Kelley, A., Smallbone, A., Zhu, D.L., and Law, C.K. 2010. Laminar flame speeds of C5-C8 n-alkanes at elevated pressures and temperatures. Presented at the 48th AIAA Aerospace Sciences Meeting Including the New Horizons Forum and Aerospace Exposition, January 4–7, Orlando, Florida.

Kumar, K., and Sung, C.J. 2007. Laminar flame speeds and extinction limits of preheated n-decane/O_2/N_2 and n-dodecane/O_2/N_2 mixtures. *Combust. Flame*, **151**, 209–224.

Kumar, K., and Sung, C.J. 2009. Flame propagation and extinction characteristics of neat hydrocarbon surrogate fuel components. Presented at the 6th U.S. National Combustion Meeting, May 17–20, University of Michigan, Ann Arbor, MI.

Kumar, K., Sung, C.J., and Hui, X. 2009. Laminar flame speeds and extinction limits of conventional and alternative jet fuels. Presented at the 47th AIAA Aerospace Sciences Meeting including The New Horizons Forum and Aerospace Exposition, Jan. 5–8, Orlando, Florida.

Kwon, S., Tseng, L.K., and Faeth, G.M. 1992. Laminar burning velocities and transition to unstable flames in $H_2/O_2/N_2$ and $C_3H_8/O_2/N_2$ mixtures. *Combust. Flame*, **90**, 230–246.

Markstein, G.H. 1964. *Nonsteady Flame Propagation*, Pergamon Press, New York.

Natelson, R.H., Kurman, M.S., Miller, D.L., and Cernansky, N.P. 2008. Oxidation of alternative jet fuels and their surrogate components. Presented at the 46th AIAA Aerospaces Sciences Meeting and Exhibit, January 7–10, Reno, Nevada.

Pitz, W.J., Cernansky, N.P., Dryer, F.L., Egolfopoulos, F., Farrell, J.T., Friend, D.G., and Pitsch, H. 2007. Development of an experimental database and kinetic models for surrogate gasoline fuels. Presented at the 2007 SAE World Congress. Detroit, MI.

Qiao, L., Gu, Y., Dam, W.J.A., Oran, E.S., and Faeth, G.M. 2007. A study of the effects of diluents on near-limit H-2-air flames in microgravity at normal and reduced pressures. *Combust. Flame*, **151**, 196–208.

Qiao, L., Kim, C.H., and Faeth, G.M. 2005. Suppression effects of diluents on laminar premixed hydrogen/oxygen/nitrogen flames. *Combust. Flame*, **143**, 79–96.

Ranzi, E., Frassoldati, A., Granata, S., and Faravelli, T. 2005. Wide-range kinetic modeling study of the pyrolysis, partial oxidation, and combustion of heavy n-alkanes. *Ind. Eng. Chem. Res.*, **44**, 5170–5183.

Ronney, P.D., and Sivashinsky, G.I. 1989. A theoretical-study of propagation and extinction of nonsteady spherical flame fronts. *SIAM J. Appl. Math.*, **49**, 1029–1046.

Schulz, W.D. 1991. Oxidation products of a surrogate JP-8 fuel. *ACS Petroleum Chemistry Division Preprints*, **37**, 383–392.

Sirjean, B., Dames, E., Sheen, D.A., You, X.-Q., Sung, C., Holley, A.T., Egolfopoulos, F.N., Wang, H., Vasu, S.S., Davidson, D.F., Hanson, R.K., Pitsch, H., Bowman, C.T., Kelley, A., Law, C.K., Tsang, W., Cernansky, N.P., Miller, D.L., Violi, A., and Lindstedt, P. 2008. A high-temperature chemical kinetic model of n-alkane oxidation. JetSurF version 0.2.

Skøth-Rasmussen, M.S., Braun-Unkhoff, M., Naumann, C., and Frank, P. 2003. Experimental and numerical study of n-decane chemistry. In: VOVELLE, C. C. A. C., ed. Proceedings of the European Combustion Meeting, Oct. 25–28, Orleans, France.

Strehlow, R.A., and Savage, L.D. 1978. The concept of flame stretch. *Combust. Flame*, **31**, 209–211.

Tahtouh, T., Halter, F., and Mounaim-Rousselle, C. 2009. Measurement of laminar burning speeds and Markstein lengths using a novel methodology. *Combust. Flame*, **156**, 1735–1743.

Tseng, L.K., Ismail, M.A., and Faeth, G.M. 1993. Laminar burning velocities and Markstein numbers of flames. *Combust. Flame*, **95**, 410–426.

Violi, A., Yan, S., Eddings, E.G., Sarofim, F., Granata, S., Faravelli, T., and Ranzi, E. 2002. Experimental formulation and kinetic model for JP-8 surrogate mixtures. *Combust. Sci. Technol.*, **174**, 399–417.

Wang, Y.L., Holley, A.T., Ji, C., Egolfopoulos, F.N., Tsotsis, T.T., and Curran, H.J. 2009. Propagation and extinction of premixed dimethyl-ether/air flames. *Proc. Combust. Inst.*, **32**, 1035–1042.

Westbrook, C.K., Pitz, W.J., Herbinet, O., Curran, H.J., and Silke, E.J. 2009. A comprehensive detailed chemical kinetic reaction mechanism for combustion of n-alkane hydrocarbons from n-octane to n-hexadecane. *Combust. Flame*, **156**, 181–199.

You, X.Q., Egolfopoulos, F.N., and Wang, H. 2009. Detailed and simplified kinetic models of n-dodecane oxidation: The role of fuel cracking in aliphatic hydrocarbon combustion. *Proc. Combust. Inst.*, **32**, 403–410.

Zhao, Z., Kazakov, J., Li, A., Dryer, F.L., and Zeppieri, S.P. 2005. Burning velocities and a high-temperature skeletal kinetic model for n-decane. *Combust. Sci. Technol.*, **177**, 89–106.